

# Polygonal orbital path of quantum gravity

Farid Abrari

1400 Woodeden Dr, Mississauga, Ont, L5H 2T9, Canada

farid.abrari@gmail.com

July 2, 2021

## Abstract

The quantum effects of gravity become apparent when particles of sufficiently small mass are located in the gravitational field of a large body of mass. In such conditions, the particles would experience the stepwise variation of the gravitational field as a series of *rings* in which the gravitational strength remains constant. Consequently, in such quantized gravitational fields, the orbital path of the particles would deviate from the circular path of the smooth classical gravity. In this article it is shown that under quantum effects of gravity, the path of an orbiting particle would look like a polygon with rounded vertices - similar to those of Saturn's hexagon. The side-count of such polygonal paths is shown to be a direct function of the width of the ring of constant gravity, which itself is a direct function of the mass of the orbiting particle. In the case of the polygonal paths of large side-count, each rounded vertex and its pair of immediate connecting edges, constitute a parabolic trajectory that the particle takes while traversing the width of the ring of constant gravity. The parabolic path of the particle is such that it gets tangent to the boundaries of the ring of constant gravity at two altitude extremes. In one extreme, when the path is tangent to the circle of high altitude, the particle velocity is less than what is required to maintain its altitude, hence, it descends afterward. In the other extreme, when the path is tangent to the circle of low altitude, the particle velocity is more than what is required to remain at that altitude, hence, it ascends afterward. This repeated altitude drops and gains results in the polygonal orbital path of the quantum gravity. The circular path of the classical mechanics emerges when the quantum effects of gravity is fully vanished by reducing the width of ring of constant gravity to zero, hence, increasing the polygon side-count unboundedly. In this limiting case, the circular path of the classical mechanics would be made of infinitesimal parabolas each fully tangent to the circular path at their vertices.

**Keywords** — Quantum Gravity, Polygon orbit, Saturn Hexagon

## 1 Background

In the quantum model of Newtonian gravity introduced in [1], the local acceleration of a particle with rest mass  $m$  falling freely in the gravitational field of a much larger body of mass  $M$  is given as:

$$\frac{GM}{R_k^2} = kc\sqrt{\frac{\bar{m}}{m}} \quad k = 1, 2, \dots \quad (1)$$

where  $k$  is understood to be the *quantum rate index*; a positive integer with the unit of  $\text{sec}^{-1}$ ,  $R$  is the distance between the masses,  $G$  is the gravitational constant and  $c$  is the speed of light. The physical interpretation of the scaling reference mass  $\bar{m} = h/Ac$  with the *estimated* rest mass of  $\bar{m} = 3.2E - 45$  (kg) was also introduced in [1, 2]. Furthermore, it was shown that for particles of *minuscule* mass, the 3D gravitational field surrounding a large body of mass  $M$  appears to be in the form of a series of *spherical shells of constant gravity* which are increasingly tight-packed as altitude drops. As shown in Fig 1, for a given pair of masses  $m$  and  $M$ , the spacing (or width) of such spherical shells (or rings in 2D) is quantized as follows:

$$x_k = R_k - R_{k+1} = \sqrt[4]{\frac{m}{\bar{m}}} \left( \sqrt{\frac{GM}{k \cdot c}} - \sqrt{\frac{GM}{(k+1) \cdot c}} \right) \quad k = 1, 2, \dots \quad (2)$$

As a convention used in this theory, the boundary circles of the ring  $k$  have radius  $R_k$  and  $R_{k+1}$ , such that at the span of  $R_{k+1} < R < R_k$  the local gravity remains constant  $g_k = GM/R_k^2$ . Due to the quantized nature of gravity  $g_k = kg_1$ , where the quantum of the gravitational acceleration that a particle of rest mass  $m$  can physically go through is numerically given by  $g_1 = c\sqrt{\bar{m}/m}$ . Also, at the distances  $R > R_1$  the gravitational force or acceleration experienced by the particle drops below  $g_1$ , hence, is experienced as zero - physically. Accordingly, the distance  $R_1 = \sqrt[4]{m/\bar{m}}\sqrt{GM}/c$  is a distance beyond which the masses  $m$  and  $M$  are not gravitationally bounded.

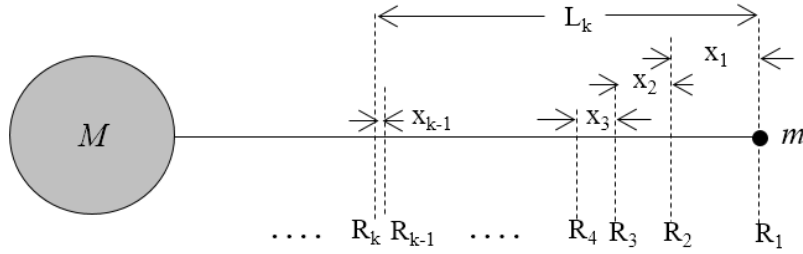


Figure 1: Rings of constant gravity around a gravitational body of mass

Due to the smooth & continuous nature of the Newtonian model of gravity, the width of such spherical shells of constant gravity is obviously zero in the classical gravity. In the latter, as a consequence, the only possible orbital trajectory on which the gravitational force acting on an orbiting particle could remain constant is that of a *perfect circle*. As discussed earlier, in the quantum model of gravity, in contrast, there exists a spatial interval within which the gravity is invariant; and as a consequence, the particle could deviate from the perfect circular path as long as its deviated trajectory is still within the ring of constant gravity. As a result, in circumstances where the quantum effects of gravity are apparent, *the stable path of orbiting particles is always a polygon rather than a circle*. It is clear that the extent of the orbital path deviations of quantum gravity from the circular path of the classical gravity is a function of the width of the ring of constant gravity. In other words, as shown in Fig 2, the wider the ring of constant gravity is, the more significant the effects of quantum gravity are; and hence, higher deviations from the perfect Newtonian circular path are expected. The side-count parameter  $B$  of a *regular polygon* and the radii ratio  $r/R$  of its inscribed to circumscribed circles are related as follows:

$$\frac{r}{R} = \cos(\theta_B) \quad (3)$$

where  $\theta_B = \pi/B$  is the angle between the edge mid-point and the immediate vertices. In Fig 2, moving from left to right, we note that as the width of the ring of constant gravity reduces, i.e. as the effect of quantum gravity diminishes, the polygonal orbital path of quantum gravity gets closer and closer to the classical Newtonian circular path. At the limit, where the quantum effects of gravity completely vanishes, and subsequently the width of constant gravity ring drops to zero,

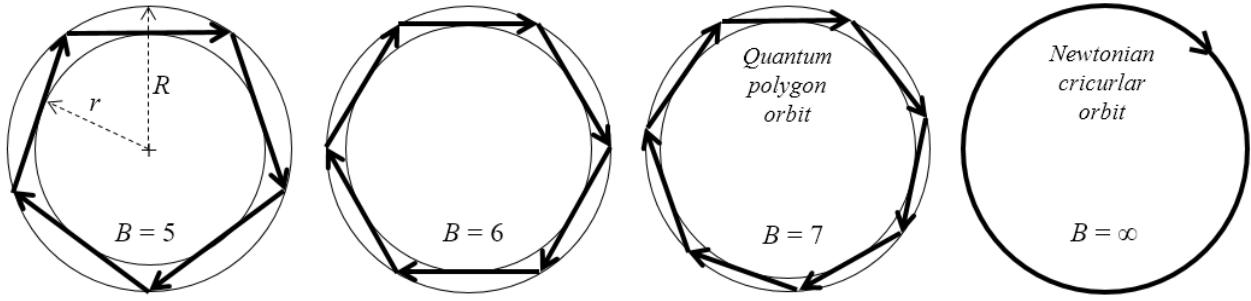


Figure 2: Quantum polygon orbit within rings of constant gravity v.s. classic circular orbit

the side-count parameter  $B \rightarrow \infty$  and the polygonal orbital path of quantum gravity reduces to the classical circular orbit.

## 2 Polygonal orbital trajectory

In this section, using the governing parameters of mass, distance, velocity and acceleration we develop a set of mathematical relationships for the polygonal orbital path of quantum gravity. As we will see, a polygonal orbital path involves a perpetual orbital transfer between two altitudes. Similar to the orbital transfer in the smooth gravitational fields [3], the mismatch between the particle's instantaneous velocity to that of the circular orbit leads to the transfer of the particle from one altitude to the other. Accordingly, for a given set of parameters, namely, the gravitational body of mass  $M$ , the distance  $R_{k+1}$  and the polygon side-count parameter  $B$ , the aim is to determine the orbiting particle mass  $m$  for which such a polygonal orbital path could be generated. A general solution for this type of problem leads to elliptical equations for which only numerical solutions exist. However, to gain insight of the physics involved, we first limit ourselves to the conditions of high distance and high polygon side-count under which an elementary analytical solution could be developed.

### 2.1 Trajectory in altitude drop

With that aim, as shown in Fig 3, let's now consider a Cartesian system of coordinates  $(x, y)$  with the unit vectors  $(\vec{i}, \vec{j})$ . Attached to the origin of this coordinate system is a large gravitating body of mass  $M$ . From Eqn 3, first an auxiliary circle of radius  $R'$  is defined as follows:

$$R' = \frac{R_{k+1}}{\cos(\pi/B)} \quad (4)$$

The space between  $R'$  and  $R_{k+1}$  is such that it accommodates a regular polygon (with point vertices) of side-count  $B$ , as shown for  $B = 6$  in Fig 3. Further, let's consider a minuscule particle of mass  $m$ , in orbit, when it is momentarily crossing the  $x$  axis at the distance  $R_k$  and angle  $\theta = 0$ . As discussed earlier, at this stage the given set of the independent variables includes  $M$ ,  $R_{k+1}$  and  $B$  only; and all other remaining *dependent variables* are yet to be determined based on the given set. As such, the instantaneous velocity of the particle is then assumed to be  $u_k < v_k$ , where  $v_k = \sqrt{g_k R_k}$  corresponds to the velocity of the particle in the classical circular orbit at radius  $R_k$ . From the Eulerian linear momentum principle, for the particle  $m$  we then write:

$$\frac{d\vec{L}}{dt} = m \frac{d\vec{v}}{dt} = m\vec{g} \quad (5)$$

where  $\vec{g} = -g_k \cos(\theta)\vec{i} - g_k \sin(\theta)\vec{j}$  is the vector of gravitational acceleration. Limiting ourselves to a large  $R_{k+1}$  and also to a large polygon side-count  $B \gg 6$ , the angle  $\theta \approx 0$  such that the

gravitational acceleration vector could be approximated, locally, by  $\vec{g} \approx -g_k \vec{i} - 0\vec{j}$ . By integration of Eqn 5 we then have the following for the velocity vector:

$$\vec{v}(t) = -g_k t \vec{i} + u_k \vec{j} = \frac{d\vec{r}}{dt} \quad (6)$$

where the particle's initial velocity vector  $u_k \vec{j}$  is used as the constant of integration. By further integration of Eqn 6 we then have the following equation for the position vector:

$$\vec{r}(t) = (-0.5g_k t^2 + R_k) \vec{i} + u_k t \vec{j} \quad (7)$$

where this time the particle's initial position vector  $R_k \vec{i}$  is used as the constant of integration. Therefore, the local  $(x, y)$  coordinates of the particle as functions of time  $t$  are given by:

$$\begin{aligned} x(t) &= -0.5g_k t^2 + R_k \\ y(t) &= u_k t \end{aligned} \quad (8)$$

Isolating time  $t$  from the first equation as:

$$t = \sqrt{\frac{2}{g_k} [R_k - x(t)]} \quad (9)$$

and substituting in the second equation we arrive at the particle's parabolic trajectory equation as:

$$y^2(t) = \beta [R_k - x(t)] \quad (10)$$

where  $\beta$  is the defining parameter of the parabola given by the following:

$$\beta = \frac{2u_k^2}{g_k} \quad (11)$$

Next, we need to find out that, starting from the higher altitude  $R_k$ , what the initial velocity  $u_k$

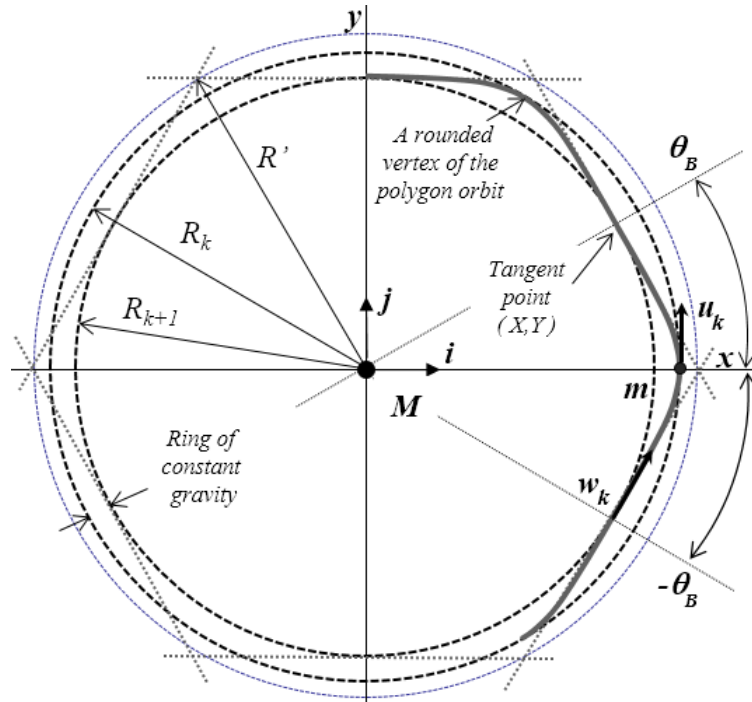


Figure 3: Polygonal path of a particle orbiting a quantum gravitational field

has to be in order to make the trajectory of the particle tangent to the lower altitude circle  $R_{k+1}$  at the given angle  $\theta = \theta_B$ . By substituting for the term  $y^2$  in the equation of circle  $x^2 + y^2 = R_{k+1}^2$  from Eqn 10 and solving for  $x$  will have:

$$x = \frac{u_k^2}{g_k} \pm \sqrt{\frac{u_k^4}{g_k^2} - \frac{2u_k^2}{g_k}R_k + R_{k+1}^2} \quad (12)$$

For the tangency condition to meet, however, the term under the square root needs to be zero. This first leads to a relationship for the initial velocity at the higher altitude  $R_k$  as follows:

$$u_k = \sqrt{v_k^2 - g_k \sqrt{R_k^2 - R_{k+1}^2}} \quad (13)$$

and then a relationship for the  $R_k$  in terms of  $\beta$  and  $R_{k+1}$  as follows:

$$R_k = \frac{R_{k+1}^2 + 0.25\beta^2}{\beta} \quad (14)$$

It is evident that the  $(X, Y)$  coordinates of the point of tangency in terms of  $R_{k+1}$  and  $B$  are given by  $(R_{k+1} \cos(\theta_B), R_{k+1} \sin(\theta_B))$ . The same coordinates are also obtained in terms of velocity  $u_k$  and acceleration  $g_k$ , first from Eqn 12 for  $X$  and subsequently from Eqn 10 for  $Y$  as follows:

$$X = R_{k+1} \cos(\theta_B) = \frac{u_k^2}{g_k} = 0.5\beta \quad (15)$$

$$Y = R_{k+1} \sin(\theta_B) = \sqrt{\frac{2u_k^2}{g_k}(R_k - \frac{u_k^2}{g_k})}$$

Substituting for  $x$  in Eqn 9 from above, the travel time between two points of tangency on the boundary circles  $R_k$  and  $R_{k+1}$  is obtained as:

$$T = \sqrt{\frac{2}{g_k}(R_k - \frac{u_k^2}{g_k})} \quad (16)$$

Finally, knowing the travel time from above the velocity of the particle when it reaches to the point of tangency at  $R_{k+1}$  is obtained from Eqn 6 as:

$$w_k = \sqrt{2v_k^2 - u_k^2} \quad (17)$$

We now note that as the effects of quantum gravity reduces, i.e. the width of ring of constant gravity reduces to zero as  $R_k \rightarrow R_{k+1}$ , both velocities  $u_k$  and  $w_k$  from Eqns 13 and 17 approach to that of the circular orbit  $v_k$  - as expected. Moreover, at this limiting condition  $\beta \rightarrow 2R_k$  and with that the parabolic trajectory of Eqn 10  $\rightarrow y^2 + x^2 = R_k^2$ .

## 2.2 Trajectory in altitude gain

While intuitive, we now need to show that the particle  $m$ , starting with the initial velocity  $w_k$  at the low altitude  $R_{k+1}$ , will follow the same parabolic trajectory and reach to the high altitude  $R_k$  with the velocity of  $u_k$ . This means the particle will end up with the exact initial conditions of the previous section. Due to the symmetry, this in turn indicates that from that point on the particle will go through a repeatable polygonal orbital path around the gravitating object  $M$ . Note that this is valid only if  $B$  is an integer number, as for non-integer values the polygon will not be closed and the particle will experience precession as it orbits the body. Therefore, by integration of Eqn 5 for the velocity vector we now have:

$$\vec{v}(t) = [-g_k t + w_k \sin(\theta_B)] \vec{i} + w_k \cos(\theta_B) \vec{j} = \frac{d\vec{r}}{dt} \quad (18)$$

where this time, as shown in Fig 3 in the 4th quadrant, the initial velocity vector  $-w_k \sin(\theta_B) \vec{i} + w_k \cos(\theta_B) \vec{j}$  is used as the constant of integration. Note that in this case  $\theta_B < 0$ . By further integration of Eqn 18, but this time using the initial position vector  $R_{k+1} \cos(\theta_B) \vec{i} + R_{k+1} \sin(\theta_B) \vec{j}$  as the constant of integration, we will arrive at the following equations for the local  $(x, y)$  coordinates of the particle when it is gaining altitude from  $R_{k+1}$  to  $R_k$ :

$$\begin{aligned} x(t) &= R_{k+1} \cos(\theta_B) - w_k \sin(\theta_B)t - 0.5g_k t^2 \\ y(t) &= R_{k+1} \sin(\theta_B) + w_k \cos(\theta_B)t \end{aligned} \quad (19)$$

Now the remaining task is to show these equations represent an *identical* parabola to that of Eqn 10, obtained for the particle when it was losing altitude from  $R_k$  to  $R_{k+1}$ . To this aim, from one hand, by substituting for  $x$  in Eqn 10 from above and simplifying we have:

$$y^2(t) = (\beta R_k - \beta R_{k+1} \cos(\theta_B)) + \beta w_k \sin(\theta_B)t + 0.5\beta g_k t^2 \quad (20)$$

and on the other hand, by squaring the term for  $y$  from Eqn 19 we have:

$$y^2(t) = R_{k+1}^2 \sin^2(\theta_B) + 2R_{k+1}w_k \sin(\theta_B) \cos(\theta_B)t + w_k^2 \cos^2(\theta_B)t^2 \quad (21)$$

For the particle trajectories in both scenarios (of losing and gaining altitude) be part of the *same* parabola of Eqn 10 we should then have a term by term equivalency between the Eqns 20 and 21. This means the following relationships need to hold true:

$$\begin{aligned} \beta[R_k - R_{k+1} \cos(\theta_B)] &= R_{k+1}^2 \sin^2(\theta_B) \\ \beta &= 2R_{k+1} \cos(\theta_B) \\ 0.5\beta g_k &= w_k^2 \cos^2(\theta_B) \end{aligned} \quad (22)$$

The first term is simply arrived by inserting the coordinates  $(X, Y)$  of the point of tangency in the parabola Eqn 10. The second equation was previously seen in Eqn 15. For the third equation, by substituting  $v_k^2 = g_k R_k$  and  $u_k^2 = 0.5g_k \beta$  (from Eqn 15) in Eqn 17 we arrive at:

$$w_k^2 = \beta g_k \left( \frac{2R_k}{\beta} - \frac{1}{2} \right) \quad (23)$$

Now by substituting for  $R_k$  from Eqn 14 and simplifying we arrive at:

$$w_k^2 = \beta g_k \left( \frac{4R_{k+1}^2}{2\beta^2} \right) \quad (24)$$

from which we arrive at  $0.5\beta g_k = w_k^2 \cos^2(\theta_B)$  by recalling that  $\beta = 2R_{k+1} \cos(\theta_B)$ . With this we then conclude that indeed the particle's trajectory in both ascending to the higher altitude  $R_k$  and descending to the lower altitude  $R_{k+1}$  are symmetric and segments of the same parabola. We further conclude that for an integer side-count parameter  $B$ , the quantum polygonal path will be closed and fully stable (repeatable).

### 3 Solution strategy

Based on the equations developed in the previous sections, we now describe a procedure for calculation of the polygonal orbit under the quantum gravity conditions. Recall that the given set of the independent variables are the mass  $M$  of the gravitating body, the distance  $R_{k+1}$  of the orbiting particle and the side-count parameter  $B$  of the polygon for which we desire to do the calculation. Using the latter two parameters  $R_{k+1}$  and  $B$ , first we determine  $\beta$  from Eqn 15. Knowing  $\beta$  and  $R_{k+1}$  then determine  $R_k$  from Eqn 14. In order to determine the mass of the particle under which

the quantum effects of gravity become apparent under the given set of parameters, from Eqn 1 first we note:

$$\frac{GM}{R_k^2 c} \sqrt{\frac{m}{\bar{m}}} + 1 = \frac{GM}{R_{k+1}^2 c} \sqrt{\frac{m}{\bar{m}}} \quad (25)$$

Knowing all parameters in Eqn 25, except the particle mass  $m$ , we now solve for the latter to arrive at:

$$m = \left( \frac{c}{GM} \times \frac{R_{k+1}^2 R_k^2}{R_k^2 - R_{k+1}^2} \right)^2 \bar{m} \quad (26)$$

Knowing  $m$  and  $R_k$ , the quantum rate index  $k$  will be calculated from:

$$k = \frac{GM}{R_k^2 c} \sqrt{\frac{m}{\bar{m}}} \quad (27)$$

Knowing  $k$ , the gravitational acceleration is obtained next:

$$g_k = kc \sqrt{\frac{\bar{m}}{m}} \quad (28)$$

The particle velocity at the high and low altitudes are then calculated from the Eqn's 13 and 17, respectively. Finally, the time  $T$  of one ascend (or descend) is calculated from Eqn 16 and then multiplied by a factor of  $2B$  to arrive at the total time of one full orbit.

Trajectories obtained from such calculations are shown in Figs 4-6 for the polygon side-count parameters  $B = 4$ ,  $B = 4.5$  and  $B = 5$ . All coordinates are normalized to  $R_k$ , limiting the graphs boundaries to  $[-1, 1]$  for ease of comparison. Note that how the increase of the polygon side-count parameter  $B$  from 4 to 5 reduces the quantum effects of gravity by reducing the width of ring of constant gravity. As discussed before, the classical circular path would emerge from this by increasing  $B \rightarrow \infty$  and reducing the width of gravity ring to zero. Also note that for a non-integer side-count parameter the polygonal path will not be closed and hence the particle will have a precessional orbital path, as shown in Fig 5. Finally, as previously mentioned, the closed form equations developed in this article is mostly valid local to the polygon vertices where the gravitational acceleration vector  $-g_k \vec{i}$  is nearly valid. Therefore, the entire polygonal trajectories of small side count (like that of Saturn hexagon with  $B = 6$ ) cannot be adequately modeled using these closed form solutions and numerical procedures are required.

## 4 Conclusion

It was shown that the trajectory of a particle orbiting a large gravitational body of mass would deviate from the classical circular path if the particle mass is sufficiently small to exhibit quantum effects of gravity. In such conditions, the stable orbital path of the particle would be a closed polygon; with such a side count that could geometrically fit within a ring of constant gravity. For particles of larger mass, where quantum effects of gravity are vanished, the width of rings wherein gravity remains constant is reduced to zero. The latter increases the side count of polygon to infinity; generating the classical circular path. It is hypothesized that Saturn's North Pole hexagon is a manifestation of quantum effects of gravity.

## References

- [1] F. Abrari, 'Quantum description of Newtonian gravity', <https://viXra.org/abs/2107.0004>
- [2] F. Abrari, 'Combined theory of Special Relativity and Quantum Mechanics', <https://viXra.org/abs/2106.0167>

- [3] W. Hohmann, 'The attainability of heavenly bodies', NASA technical translation F-44, Nov 1980

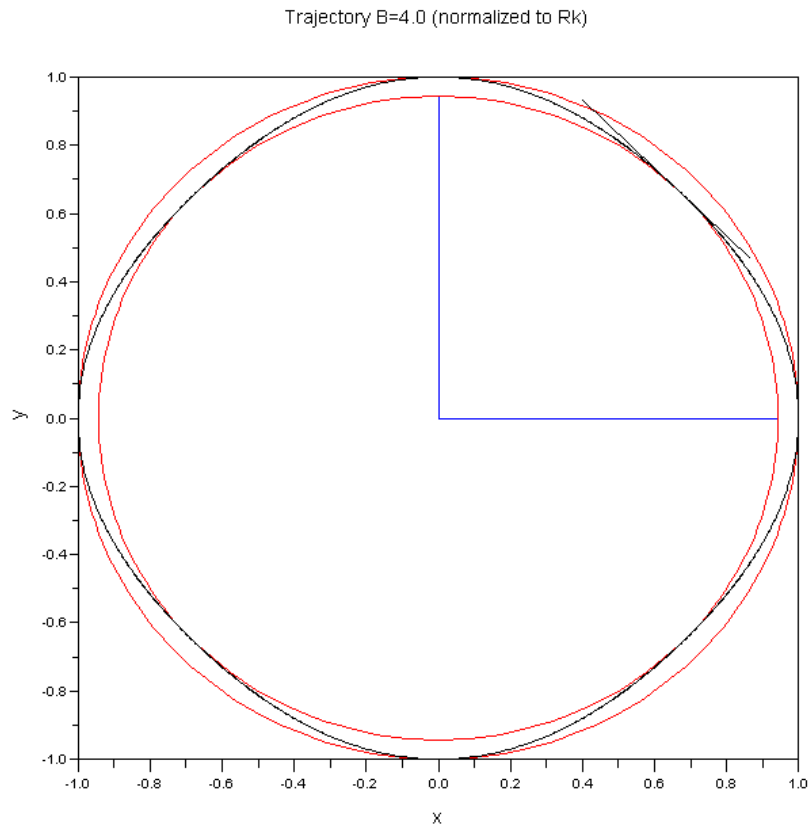


Figure 4: Normalized trajectory B=4

Trajectory B=4.5 (normalized to Rk)

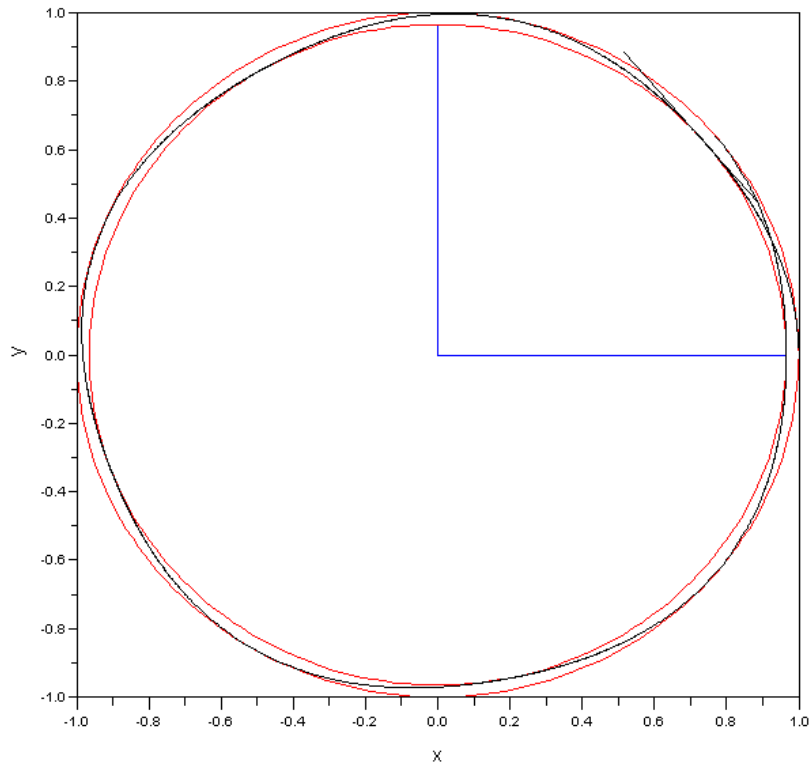


Figure 5: Normalized trajectory B=4.5 (a precessional orbit)

Trajectory B=5.0 (normalized to Rk)

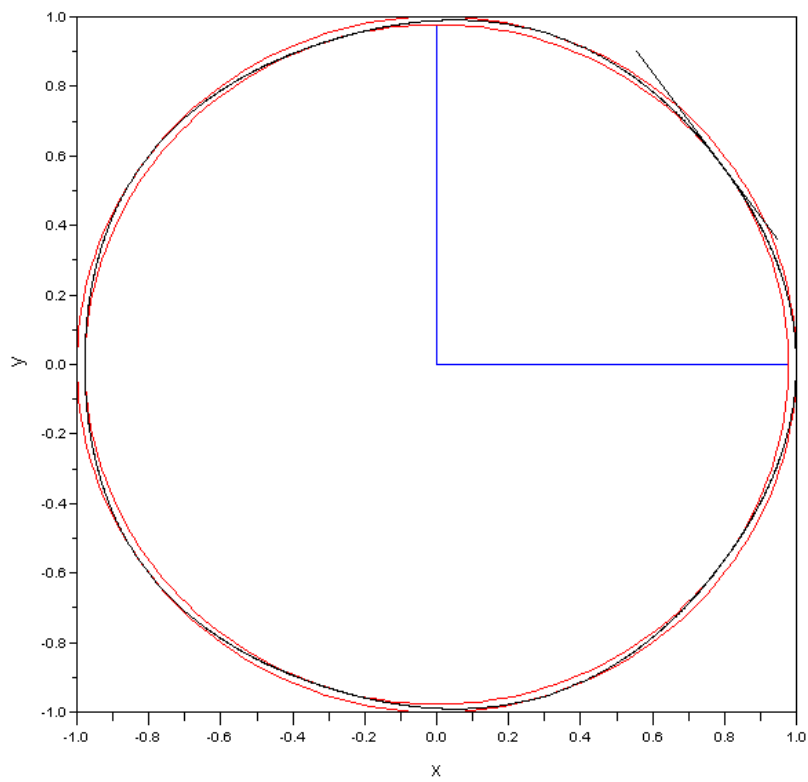


Figure 6: Normalized trajectory B=5